5-2013

Micro-Electro-Mechanical Systems (MEMS) Integrated Frequency Reconfigurable Antenna

Abdul Zohur
Utah State University

MICRO-ELECTRO-MECHANICAL SYSTEMS (MEMS) INTEGRATED FREQUENCY RECONFIGURABLE ANTENNA

by

Abdul Zohur

A thesis submitted in partial fulfillment
of the requirements for the degree

of

MASTER OF SCIENCE

in

Electrical Engineering

Approved:

Dr. Bedri Cetiner Major Professor	Dr. Doran Baker Committee Member
Dr. Edmund Spencer Committee Member	Dr. Mark R. McLellan Vice President for Research and Dean of the School of Graduate Studies

UTAH STATE UNIVERSITY
Logan, Utah

2013

Abstract

Micro-Electro-Mechanical Systems (MEMS) Integrated Frequency Reconfigurable Antenna

by

Abdul Zohur, Master of Science

Utah State University, 2013

Major Professor: Dr. Bedri Cetiner
Department: Electrical and Computer Engineering

In this paper, the design, analysis, and characterization of reconfigurable antennas based on radio frequency micro-electro-mechanical systems (RF MEMS) operating in the United States' public safety (PS) bands are presented. The design methodology of these antennas, which are different from the normal antenna design, is also reported. In this thesis, two electrically small reconfigurable antenna designs have been presented, with two and three modes of operation, and central frequencies of 718 and 4960 MHz and of 857,809 and 4960 MHz, respectively. The maximum frequency tunable ratio achieved in these designs is 7. The reconfigurability between the modes is achieved by one and three RF MEMS switches in all three designs. These switches enable a change in the length of the current flow path, thereby changing the resonance frequencies. The measurement results for impedance and radiation characteristics of the fabricated antennas prototypes are also presented, and agree reasonably well with the simulations results from An-soft HFSS.

(36 pages)

Public Abstract

Micro-Electro-Mechanical Systems (MEMS) Integrated Frequency Reconfigurable Antenna

by

Abdul Zohur, Master of Science

Utah State University, 2013

Major Professor: Dr. Bedri Cetiner
Department: Electrical and Computer Engineering

This thesis investigates the concept of reconfigurability of an antenna's properties, such as frequency, radiation pattern, and polarization, for a planar inverted-F antenna (PIFA), by the use of radio frequency micro-electro-mechanical system (RF MEMS) switches. This research work has been conducted at the Micro/Nano Electro Mechanical Systems (μN_eMS) Laboratory at Utah State University. In this thesis, two electrically small frequency reconfigurable antenna designs have been presented with two and three modes of operation with central frequencies of 718 and 4960 MHz and of 857,809 and 4960 MHz, respectively. The maximum frequency tunable ratio achieved in these designs is 7. The reconfigurability between the modes is achieved by one and three RF MEMS switches in both the designs. These switches enable changing the length of the current flow path; thereby the resonance frequencies are changed. The measurement results for impedance and radiation characteristics of the fabricated antennas prototypes are also presented, which agree reasonably well with the simulations.

To my beloved parents and family members, Saboor Sahely, and all other family members and friends.

Acknowledgments

I would like to convey my best regards to my advisor and instructor, Dr. Bedri A. Cetiner, for all of his support. He gave much needed help during the difficult times and I credit him with making this happen. Thanks to Hema Swaroop Mopidevi, for giving so much of his time to this project, through suggestions, ideas, corrections, and responses to all of my dumb requests and questions. He also taught me how to fabricate, measure, and accomplish many other things. Additional thanks go to Dr. Kaynar, a visiting professor from Turkey, who offered help in soldering and assembling the design. Thanks to my committee members, Dr. Doran Baker and Dr. Edmund Spencer. Dr. Baker believed in me and extended his support, and Dr. Spencer provided many consultations and offered supportive ideas. I would like to give my appreciation and express my highest regards for my cousin Saboor Sahely, who sponsored me from Afghanistan for this program. I would like to extend my gratitude for all of his kindness in preparing me with whatever I needed; without such things, I could not have made this happen. Also, thanks go to his kind wife, Kristine Sahely, who always made certain that I had my needs for school, including delicious food. In general, I would like to thank their lovely family, especially Jessica Sahely Bigler, who helped me with my English in critical times. Finally, I would like to thank another cousin, Abdul Shour Askar, and his kind family for their encouragement that they gave me along the way. They supported me and sustained me with their many meals. A huge thank you goes to my super kind and lovely wife, who is always supporting me, and giving me the morale to make things happen. For her constant love that made me stronger in reaching my goals in my life, thanks.

Abdul Zohur

Contents

List of Tables

List of Figures

Acronyms

Bw	Bandwidth
FRA	Frequency Reconfigurable Antenna
HFSS	High Frequency Structure Simulator
MEMS	Micro-Electro-Mechanical Systems
PIN	Positive Intrinsic Negative
MRA	Multi-Functional Reconfigurable Antenna
PIFA	Planar Inverted F Antenna
PS	Public Safety
RF	Radio Frequency
US	United States
STG	Small T-Shaped Ground
FET	Field Efect Transistor
SOL	Short Open Load

Chapter 1

Introduction

Antennas are the backbone and critical components of today's wireless communication system. There are many types of antennas; however, reconfigurability for antennas provides an additional level of functionality to the system. In this fast-paced technological era, the need for wireless communication systems (voice, data, and video) is rapidly increasing. To satisfy this need, a robust communication system – which can be benefitted by the antennas with adaptability – is desired. In this scenario, multi-functional reconfigurable antennas serve beneficially, by providing interoperable communication between users. Multi-functional Reconfigurable Antennas (MRA) [1-4] are antennas which can dynamically reconfigure in frequency, beam tilt, polarization, etc. Micro-electro-mechanical Systems (MEMS) [1] switches were selected as the building blocks for the MRA in this work. MEMS switches dynamically change the geometry of an MRA which thereby facilitates it to reconfigure in frequency, maximum direction of radiation, polarization, etc. RF MEMS switches, due to their higher isolation and lower insertion losses than PIN or field-effect transistor (FET) diode switches, are a good choice for MRAs.

The objective of this research is to design the frequency-reconfigurable electrically-small antenna, integrated with MEMS switches to satisfy the needs of today's robust communication system discussed above. This antenna should be able to switch its operational frequency between the PS bands 700 and 4900 MHz. With the rapid development of the wireless communication system, a compact and low-profile antenna is highly desirable. For this purpose, a planar inverted-F antenna (PIFA), as presented in this thesis, is best suited because of its low profile, compactness, and built-in structure. A legacy PIFA consists of a ground plane, top radiation patch with an inner conductor of coaxial cable to feed the RF energy, and a shorting wall to ground the top patch metal. The general technique to

broaden the bandwidth in a PIFA is to raise the height of the shorting plate.

In this thesis, a combination of bandwidth enhancement techniques (T-shaped ground plane [2], tapering the top patch [3], capacitively coupled feed method [4]) have been used to broaden the narrow bandwidth (BW) of a legacy PIFA. The reduction of the size of this antenna has been accomplished by using a meandered metallization on the ground plane which is a part of the T-shape ground plane. The flow of this research is categorized into three major parts. Initially, the design of a frequency reconfigurable MEMS integrated planer inverted-F antenna (PIFA), with two modes of operation, for the United States' public safety bands was implemented. It was designed in a moderate size, as explained in the following section. Second, an electrically-small frequency reconfigurable planar inverted F antenna (PIFA) was integrated with a single MEMS switch, to switch between the two US PS bands, 718 MHz and 4960 MHz, as explained in detail in Chapter 2. And lastly, another electrically-small frequency reconfigurable planar inverted-F antenna (PIFA) was integrated with three MEMS switches to reconfigure between the three US PS bands: 764-776 MHz, 806-825 MHz, and 4900 MHz, as explained in detail in Chapter 3.

Chapter 2

MEMS Integrated Frequency Reconfigurable for PS Application PIFA

2.1 Antenna Geometry

The geometry, shown in Fig. 2.1, is a frequency reconfigurable antenna capable of switching between the Public Safety bands 778 - 838 MHz (mode 1) and 4900 MHz (mode 2). The geometry shows two antennas fed by a single coaxial feed. The first antenna, which is responsible for mode 1 operation, is a capacitively fed PIFA with a reconfigurable T-shaped ground metallization and top patch. The second antenna is a capacitive loaded, directly fed PIFA, and is responsible for mode 2. A separate small T-shaped ground (STG) is located as a third layer between the top patch and the reconfigurable ground plane and is the major radiating element for mode 2. The second antenna is connected to, or isolated from, the first antenna by using three RF MEMS switches (two on the top patch and one on the ground plane), as shown in Fig. 2.1. An-soft HFSS v.11 is used in designing this frequency reconfigurable PIFA with three layers: the top patch layer, STG layer, and the ground plane layer. The STG is designed to operate in the 4.9 GHz band and is located at an optimum height of 2.975 mm from the ground plane. The radiating metal of the STG is located underneath the STG substrate. Also, the metal from regions 1 and 2 from the ground plane is peeled off to obtain the proper shape which, in turn, helps to avoid the coupling between the STG and the reconfigurable ground plane. The STG is shorted to the capacitor patch through a shorting plane to form a PIFA configuration.

2.2 Critical Design Parameters

The critical design parameters, shown in Fig. 2.1, are as follows: L_g and W_g length and width of the reconfigurable T-shape ground plane; A and B dimensions of the tapering;

L_c and W_c, length and width of the capacitive feed and loading plate; L_p and W_p, length and width of the top patch element; W_t, width of the T-shape; L_1 and L_2, length and width of the pole-structure; L_3, width of the step which connects the meander to T-shaped arm (Fig. 2.2(b)); L_4, width of the meander responsible for mode 1 operation; L_m and W_m, length and width of the STG; W_{mp} and L_{mp}, width and length of the pole structure of STG; l_g is the width of the bottom rectangle of STG; W_1 and h_1, width and height of the shorting plane which connects top patch element with the reconfigurable T-shape ground plane; and W_2 and h_2, width and height of the shorting plane which connects the capacitor plate to the STG.

2.3 Parametric Analyses

Parametric analyses have been conducted on all the parameters. The most nearly optimal values were chosen and optimized simultaneously to achieve acceptable results in both modes of operation. One of the critical parameters is the taper on the top patch, which controls the volume of the antenna and the impedance matching in mode 1. The near optimal values for dimensions A and B take into account the amount of tapering as is evident from Fig. 2.1 and Fig. 2.2. Another important parameter is the top patch length. As the length of the top patch increases to some optimum value, the impedance matching is improved in both modes of operation. When the width of the pole-structure, represented by L_2 in Fig. 2.2(b), increases, it improves the impedance matching of mode1 at the cost of impedance matching of mode 2. This means that there is a best design value for L_2 (= 41.78 mm) in which both the modes have acceptable impedance matching. The shorting wall position also plays an important role in controlling the matching levels of both modes of operation. In addition to this, parametric analyses have been performed on STG (responsible for mode 2 operation) to achieve the desired 4.9 GHz band. The width W_{mp} plays an important role in improving the impedance match in mode 2, whereas the length L_{mp} is instrumental in tuning the frequency of operation. Both modes of operation are jointly optimized and the final results are shown in the following section.

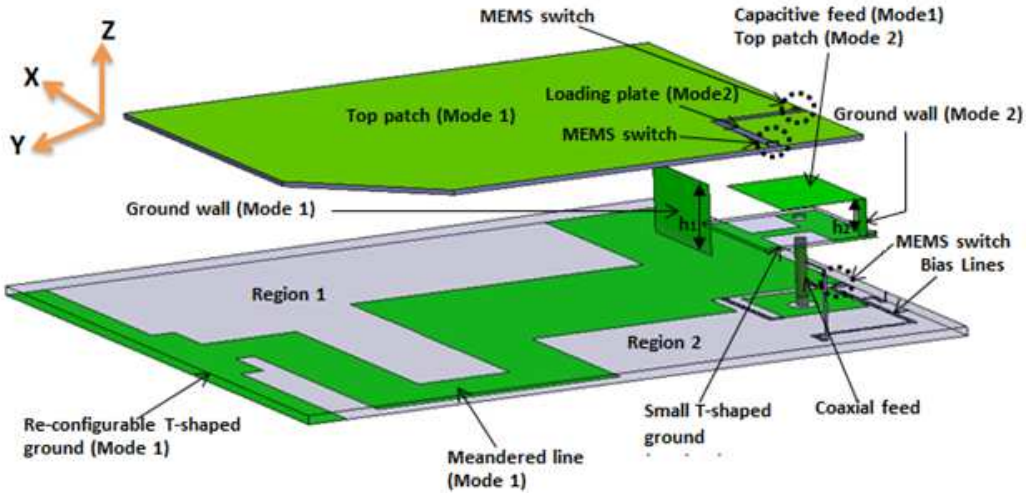

Fig. 2.1: The 3D view of the proposed reconfigurable PIFA.

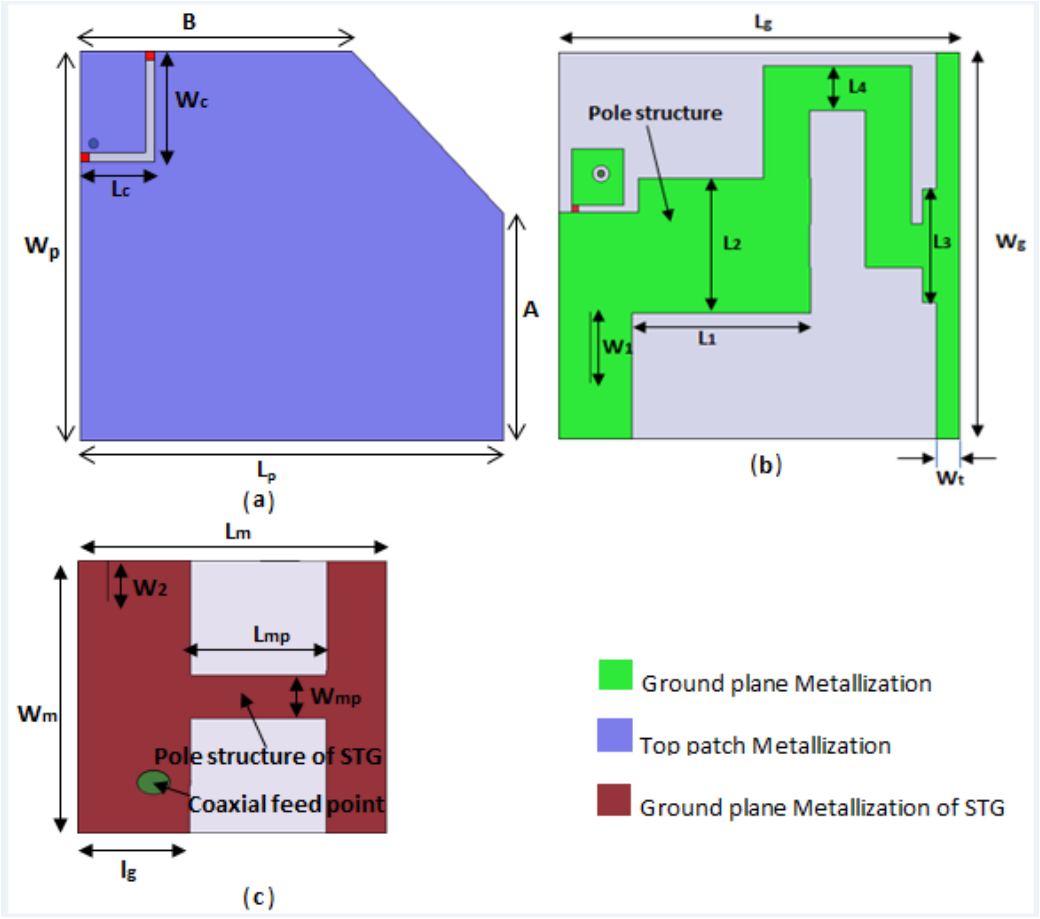

Fig. 2.2: The layout of the antenna parts: (a) top patch, (b) reconfigurable T-shape ground plane, (c) small T-shape ground.

2.4 Optimized Design

Finally, all the parameters mentioned above are jointly optimized to achieve acceptable performance in both modes of operation. The final optimum values for the parameters in both modes of operation are: A = 63.023 mm, B = 74.598 mm, L_2 (pole-width) = 41.78 mm, L_p = 95.56 mm, shorting wall dimensions (W_1 = 22.22 mm; h_1 = 12 mm), STG dimensions (L_m = 20.56 mm; W_m = 25 mm, height = 5 mm from the reconfigurable T-shape ground plane to the bottom of STG), and the dimensions of second shorting wall that connects the STG to the capacitive feed plate dimensions (W_2 = 3.647 mm; H_2 = 6.67 mm height measured from the bottom of the STG to the capacitive feed plate). The reflection coefficient and the radiation patterns for both the modes are shown in Figs. 2.3-2.6 below.

2.5 Future Work

As compactness of antennae is one of the major constraints of the next generation's wireless communication systems, the above design has not been fabricated because of the need of further size reduction. The next chapter explains the design of a smaller compact frequency reconfigurable antenna in detail.

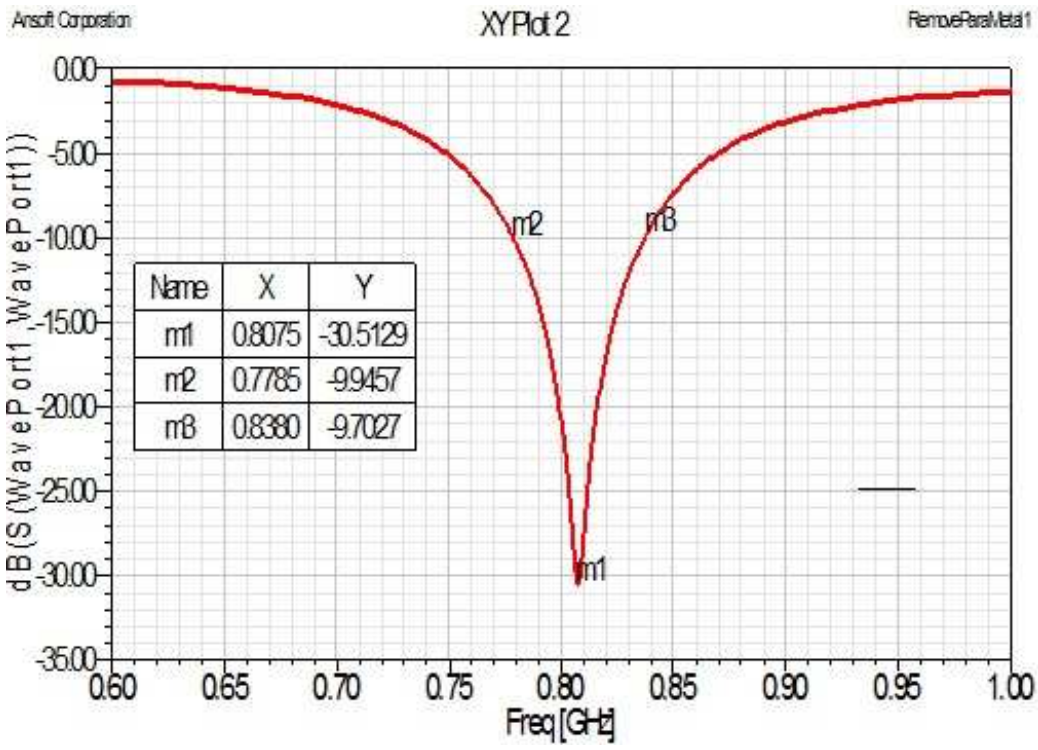

Fig. 2.3: Reflection coefficient showing the frequency band of mode 1.

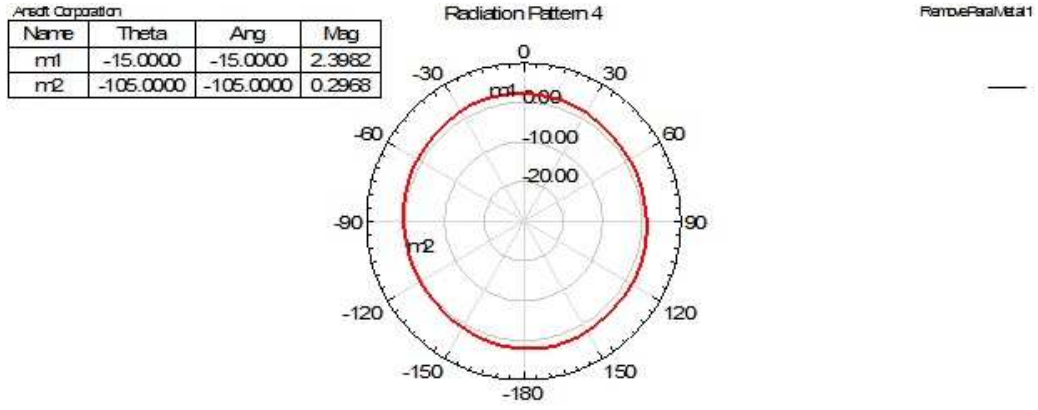

Fig. 2.4: The radiation pattern plot showing the gain values in xy plane at 780 MHz.

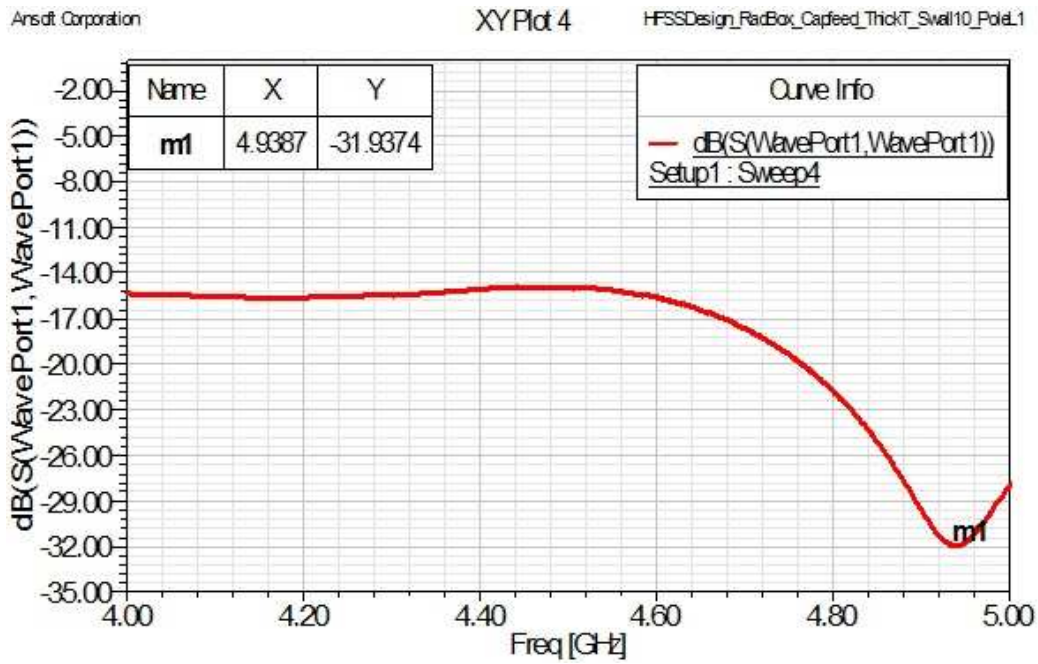

Fig. 2.5: Reflection coefficient showing the frequency band of mode 2.

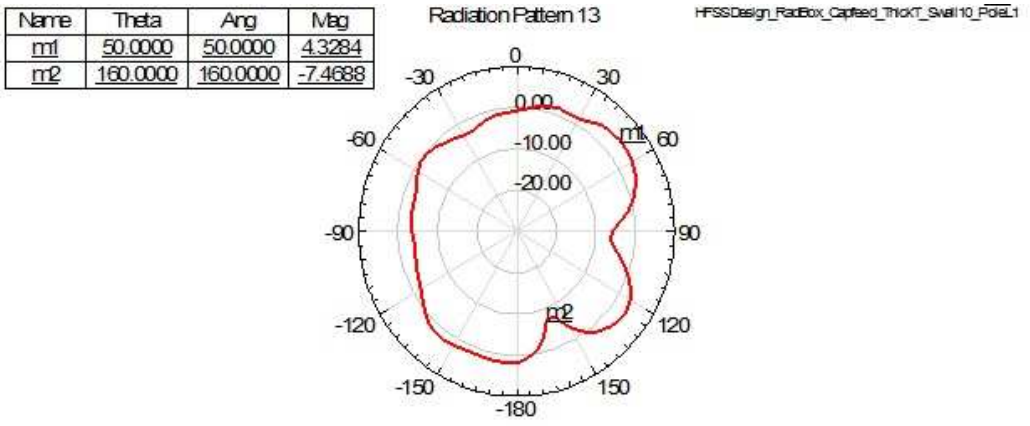

Fig. 2.6: The radiation pattern plot showing the gain values in xy plane at 4900 MHz.

Chapter 3

Electrically-Small MEMS Integrated FRA for PS Application PIFA

3.1 Antenna Architecture and Operation

As stated above, one of the most important feature of today's wireless communication system is the size of the radiator or receiver (antennas). Planar inverted-F antennas (PIFAs) are used in hand-held devices such as cellular telephones, where the size of the antenna is important. As mentioned above, a basic PIFA has less than 10% bandwidth. However, by using various bandwidth enhancement techniques, this issue can be addressed significantly (such as T-shaped ground plane [2], tapering of the top patch element [5], and capacitive feeding [4], as explained in detail below). All of these techniques combined together with the advantages of MEMS could support the United States' public safety communication system.

Interoperability between widely-spaced frequency bands enhances the effectiveness of a multi-mode, multi-band wireless communication system in improving the quality of communication. This type of robust communication is also critical when a large number of emergency responders (public safety (PS) personnel: police, firefighters, and emergency medical services) operating over different bands, need to be accommodated to deal with man-made or natural catastrophic situations. For a single antenna to be able to cover multiple frequency bands, various design approaches are used: multi-frequency antenna covering each individual band [6], a broadband antenna covering the entire frequency bandwidth (BW) [3], or a frequency reconfigurable antenna (FRA) with a narrow instantaneous operating BW that can be tuned over the entire band. When the frequency bands of operation are widely separated, it is difficult to provide a good impedance match in a multi-frequency antenna at

such distant resonances. Moreover, when the tradeoff between the separation of frequency bands and the maintenance of radiation characteristics over the bands is considered, among the three approaches, the reconfiguration approach provides an optimum solution. Planar inverted F-antennas (PIFAs) [7] are commonly used in mobile devices, where compact antennas are required. With the advantages brought by the RF MEMS technology, a MEMS integrated frequency reconfigurable PIFA would therefore become highly beneficial for emergency responders to have effective wireless communications. In this paper, an FRA, which can tune its frequency of operation between two widely spaced United States (US) PS bands (700 MHz and 4900 MHz), while at the same time maintaining a reasonable integrity in its radiation characteristics, is reported. The reconfigurability is achieved by using a single RF MEMS ohmic contact switch [8], which is integrated at a strategic location of the antenna geometry (see Fig. 3.1). The switch is used to change the path length of the current on the antenna. This, in turn, enables the antenna to tune its operating frequency band with central frequencies of 718 MHz and 4960 MHz with a tunable frequency ratio of 7.

The design of an FRA requires additional design constraints as compared with an antenna with fixed properties. The key aspect of this design methodology is to maintain the desired performance characteristics of the FRA in one mode of the operation while optimizing the parameters of the other mode of operation. In other words, the desired performance characteristics and the associated physical parameters of both modes of operation (700 MHz and 4900 MHz) need to be jointly optimized. The reconfigurable antenna presented in this paper is electrically small (lateral dimensions $\lambda/10x\lambda/10$ at $718MHz$) and accomplishes a high tunable frequency ratio when compared to similar MEMS integrated FRAs in the literature [1,5]. The working mechanism of this antenna is similar to a printed monopole although the architecture resembles the PIFA, as explained below. Measured and simulated radiation patterns and reflection coefficients of the antenna, with a reasonably good agreement between them, are also presented.

3.2 Antenna Design, Operation, and Analysis

The images and schematics of the proposed antenna are shown in Fig. 3.1 and Fig. 3.2.

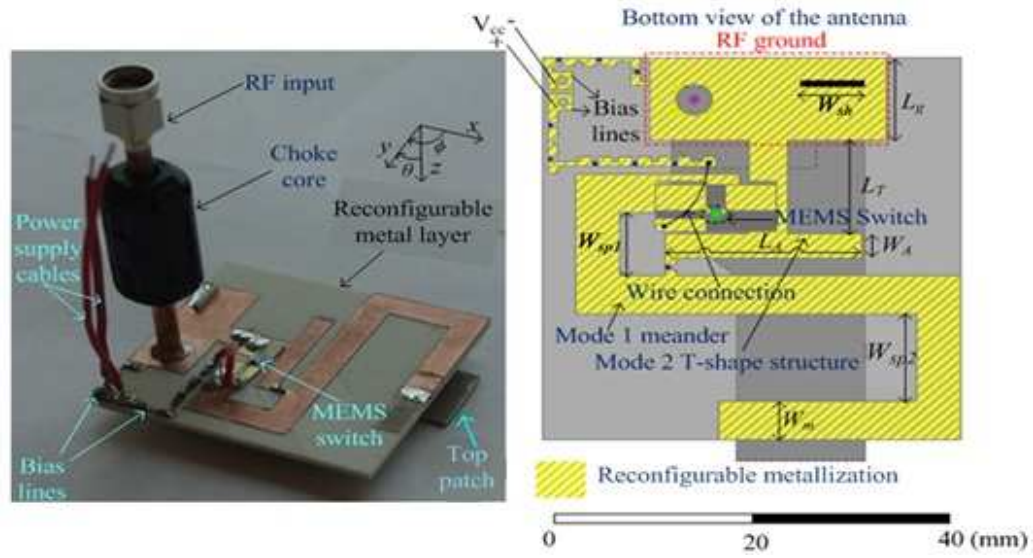

Fig. 3.1: The photographs and schematics of the RF MEMS integrated antenna depicting the critical design parameters.

The antenna is composed of two layers that are fabricated on RO4003 substrate ($\epsilon r = 3.38$, $\tan \delta = 0.002$), and air is used as the substrate between the two layers. The bottom layer, which also contains the RF MEMS switch, is used as the reconfigurable metal layer (see Fig. 3.1), and the top layer is used for the top patch (see Fig. 3.2). The antenna has two modes of operation that are centered around 718 MHz (mode 1) and 4960 MHz (mode 2). When the meander (indicated as mode 1 meander in Fig. 3.1) is connected (switch is ON) the antenna operates in mode 1, and when it is disconnected (switch is OFF) the antenna operates in mode 2. The distance between the two layers is optimized to be 5.5 mm. To accommodate the capacitive feed (shown in Fig. 3.2) in the design, which compensates for the inductance effect of the coaxial feed, a RO4003 substrate with a thickness of 0.813 mm is sandwiched by the bottom conductive plate of the capacitive feed and top patch metal of the antenna.

3.3 Design Methodology

ANSYS HFSS v13 [9] was used to perform theoretical analyses for the design. Initially, the antenna is designed to satisfy the requirements of mode 2, where T-shaped structure [2],

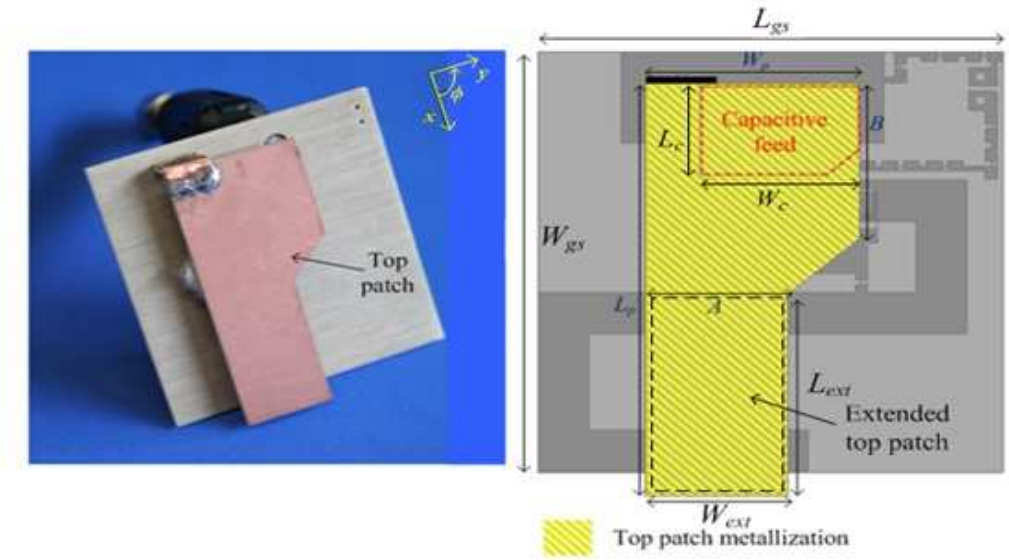

Fig. 3.2: The photographs and schematics of the RF MEMS integrated antenna depicting the critical design parameters.

tapering of the patch [3], and capacitive feeding techniques [2, 3] are employed in order to increase the BW. Then, a meander (mode 1 meander see Fig. 3.1) is introduced to reduce the resonance frequency of the antenna to 718 MHz (mode 1). The length, shape, and position of the meander are important for proper operation of the antenna. Although the meander reduces the resonance frequency significantly, it does not give a good reflection coefficient at mode 1, if not optimized jointly with other critical design parameters such as the dimensions of top patch (L_p, W_p, A, B, L_{ext}, and W_{ext}) shown in Fig. 3.1. Therefore, the antenna has been reoptimized by extending the top patch metallization (using parameters L_{ext} and W_{ext}) so that a good reflection coefficient in each mode of operation can be achieved.

3.4 Analysis and Operation

In this proposed design, the mode 1 meander and mode 2 T-shape structures are the main radiating elements (in mode 1 and mode 2, respectively) with the top patch useful in providing a good reflection coefficient in each mode of operation (mode 1 and mode 2). This explanation is supported by the simulated surface current plots of the proposed design shown in Fig. 3.3 and Fig. 3.4. The parameters L_1 (104 mm) and L_2 (19 mm), shown in

Fig. 3.3, correspond to approximately $(\lambda/4)$ resonant lengths at 700 MHz and 4.9 GHz, respectively. The RF ground shown in Fig. 3.3 is the common ground for both modes of operation.

To further explain the working mechanism of the proposed antenna, the effect of parameters L_1 and L_2 on the antenna's reflection coefficient in mode 1 and mode 2, respectively, was also studied. As shown in Fig. 3.5, when L_2 was kept (=19 mm) fixed, change in the parameter L_1 resulted in a shift in the resonant frequency f_{c1} of mode 1, with L_{11}(=104 mm), L12(=97 mm), and L_{13} (=90 mm) being $(\lambda/4)$ resonant lengths at f_{c11} (=706MHz), f_{c12} (=736MHz), and f_{c13} (=780MHz), respectively. Similarly, while L_1 was kept (=104 mm) fixed, change in the parameter L_2 resulted in a shift in the center frequency f_{c2} of mode 2, as shown in Fig. 3.6. Although the exact $(\lambda/4)$ resonant lengths at f_{c21}(=4.92GHz), f_{c22} (=5GHz), and f_{c23} (=5.07GHz) are equal to 15.25 mm, 15 mm, and 14.8 mm, respectively, the effective resonant lengths obtained from simulations are L_{21} (=19 mm), L_{22} (=16 mm), and L_{23} (=13 mm), respectively.

This is mainly due to the extended top patch coupling EM energy to the disconnected mode 1 meander, which thereby parasitically loads the mode 2 T-shape structure, due to its close proximity.

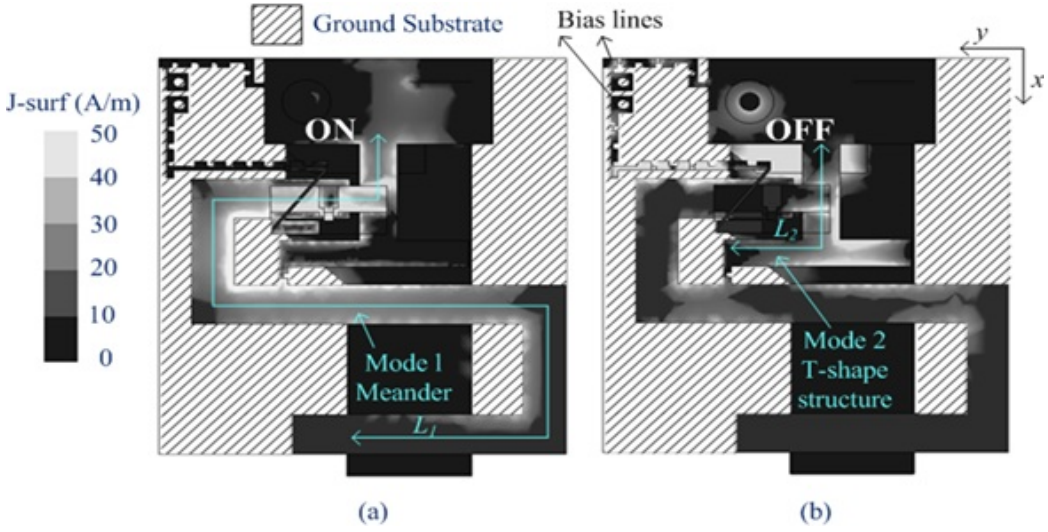

Fig. 3.3: Simulated surface current plot of the antenna along with the status of MEMS switch in (a) mode 1 and (b) mode 2.

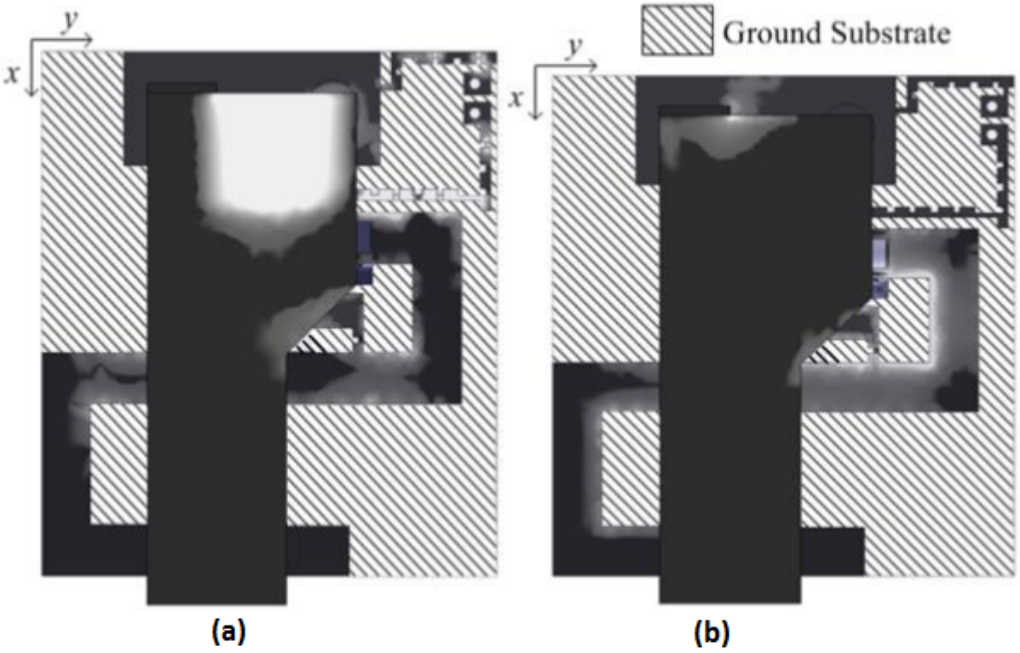

Fig. 3.4: Simulated surface current plot of the antenna top patch (a) mode 2 and (b) mode 1.

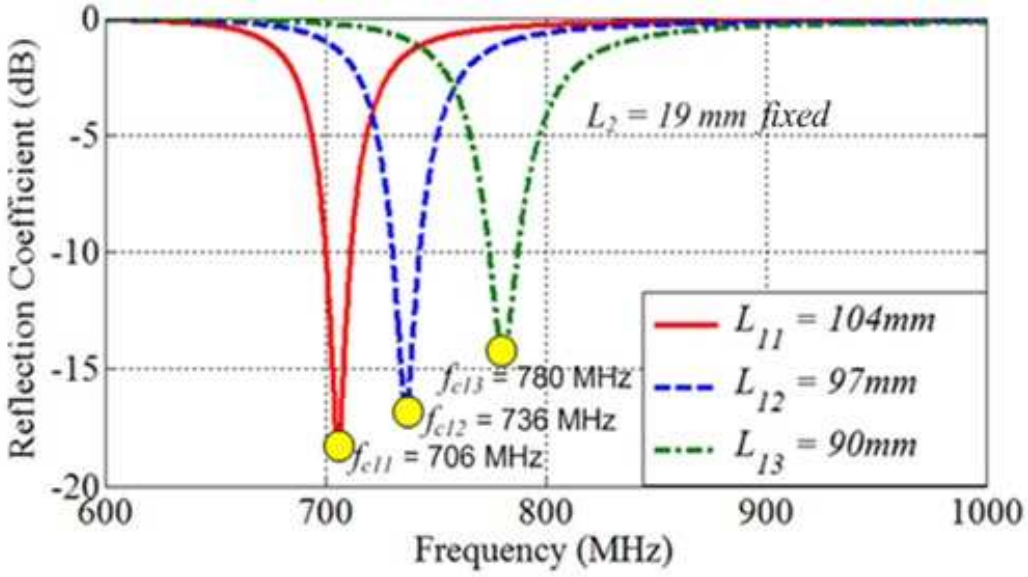

Fig. 3.5: Effect of change in parameter L2 in mode 2.

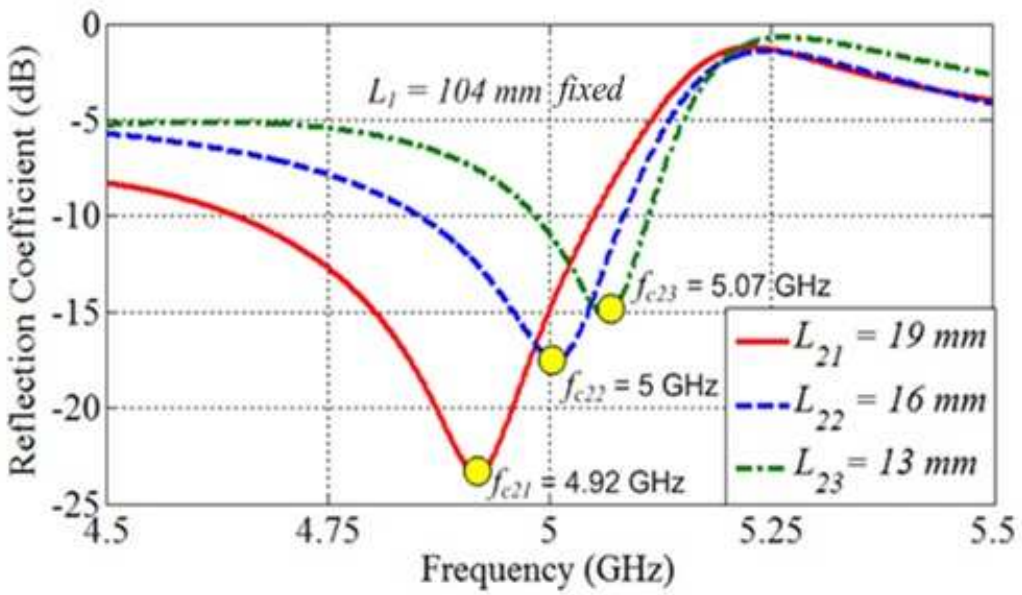

Fig. 3.6: Effect of change in parameters L1 in mode 1.

The critical design parameters for the proposed antenna are presented in Fig. 3.1 and Fig. 3.2 and also the critical design parameters for the proposed antenna are listed in Table 3.1 (all the prameters are in mm). The OFF state capacitance and ON state resistance of the RF MEMS switch are also taken into account during the design of the proposed antenna, which have significant effects on the values of the critical design parameters. Another important part of the proposed antenna design is the compensation of the effects of copper bias lines (see Fig. 3.1) used to actuate the RF MEMS switch. The two bias lines are delimited by a total of 5 SMD inductors (8 nH) and 3 SMD resistors (500 $k\Omega$) so that the bias lines have negligible effects on the antenna characteristics in both modes of operation (mode 1 and mode 2).

Table 3.1: The critical design parameters of the antenna (all dimensions are in mm).

W_{gs}	45	W_{ext}	12.8	L_g	9.8	W_{sp1}	7.5
L_{gs}	41.8	A	12.8	L_T	11	W_{sp2}	10.3
W_p	19.2	B	16.5	W_A	3.9	W_m	4.5
L_p	44	L_c	19.6	L_A	18.5	W_{sh}	6.4
L_{ext}	21.6	W_c	14.4				

3.5 Measurement Results and Discussion

The reflection coefficient of the antenna is measured using Agilent 8722ES network analyzer with one-port Short Open Load (SOL) calibration. During the measurements, Vcc = 90V, actuation voltage is used for the RF MEMS switch actuation. Figures 3.7 and 3.8 show the reflection coefficient measurement results of the fabricated antenna prototype in both modes of operation, which agree reasonably well with the simulations. The measurement results show that the antenna has a 10-dB bandwidth of 20 MHz (2.6%) and 223 MHz (4.5%) in mode 1 and mode 2, respectively. In mode 1, the fractional BW (2.6%) obtained from measurement can be considered reasonably wide [9], considering the lateral dimensions of the antenna, $\lambda/10x\lambda/10$ at 718 MHz. The Chu's limit [9] for quality factor (Q) of the antenna is given as

$$Q = 1/ka + 1/(ka)^3 \tag{3.1}$$

where $k = 2\pi/\lambda$ is the wavenumber in air and a is the radius of the smallest sphere that encloses the antenna. From Equation (3.1), the Q of the presented antenna is 14 which accounts to 7.1% as the maximum fractional BW that can be obtained with this structure. Hence, a measured fractional BW of 2.6% at 718 MHz can be considered reasonably wide for the presented antenna. Moreover, the Q obtained by taking the reciprocal of the measured fractional BW in Mode 1 is 38 which is 2.7 times the Chu's limit. To obtain the radiation patterns, the antenna prototype is placed on a rotor in the anechoic chamber and a power supply was used to actuate the single MEMS switch. The total normalized electric field intensities in xz and xy planes are shown in Figs. 3.9 and 3.10. As seen from these figures, the measured and simulated radiation patterns agree reasonably well. A dipole type radiation pattern is expected from the geometry of the main radiating elements, mode 1 meander and mode 2 T-shape structure in mode 1 and mode 2, respectively. Correspondingly, a figure of eight pattern in the xz plane, in both modes of operation (see Fig. 3.9), confirms the analysis. The null in the radiation pattern of mode 2 in $\theta = 180^\circ$ direction (in Fig. 3.9) and the compromise of radiation pattern integrity in xy plane between both modes of operation (in Fig. 3.10) is mainly due to the effect of extended top patch in

mode 2 operation as explained in section above. The differences between simulations and measurements may mainly be attributed to the obstruction of the rotor in measurement in $\theta = 180°$ direction, and the undesired radiation of the power supply cables (see Fig. 3.1). The measured directivities of the antenna obtained by averaging the 3D patterns are 2.44 dB at 710 MHz (Mode 1) and 4.01 dB at 4960 MHz (mode 2) which are quite close to the simulated results.

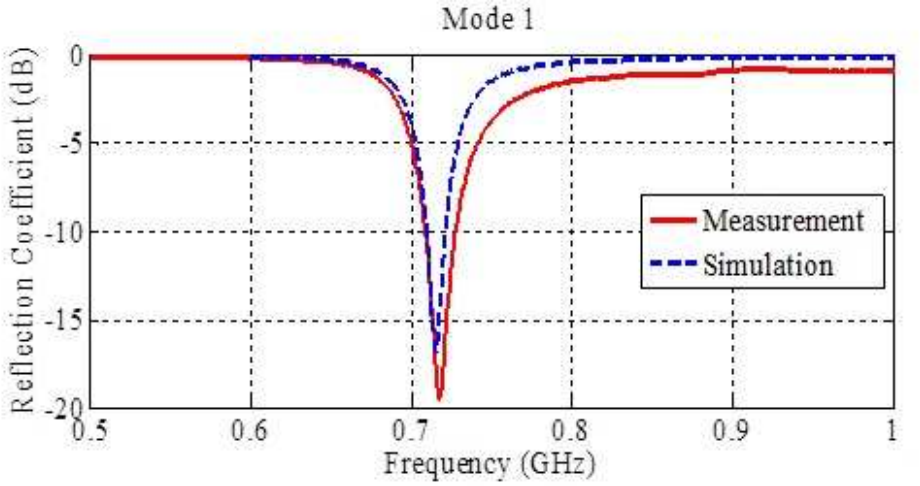

Fig. 3.7: Simulated and measured reflection coefficients of the antenna in mode 1.

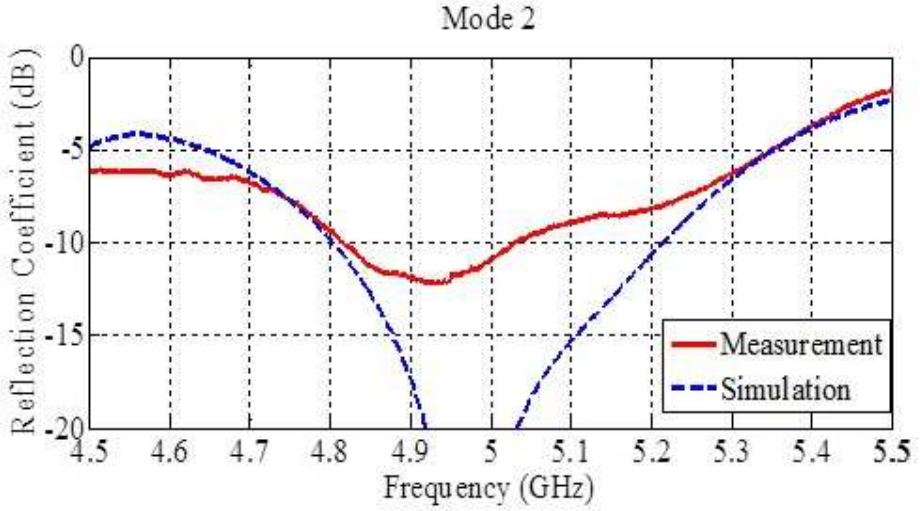

Fig. 3.8: Simulated and measured reflection coefficients of the antenna in mode 2.

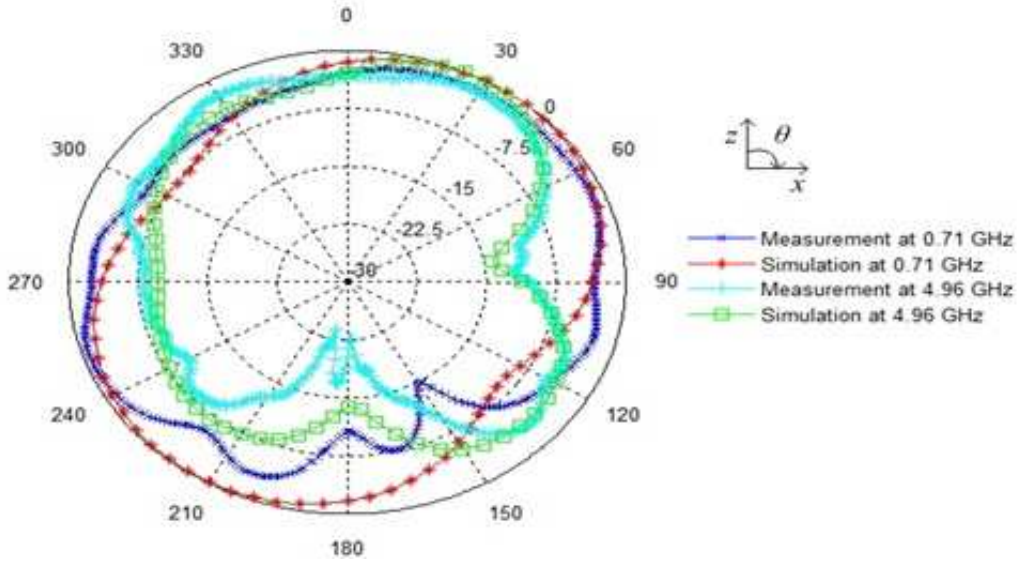

Fig. 3.9: Simulated and measured total normalized electric field intensities of the antenna in xz plane.

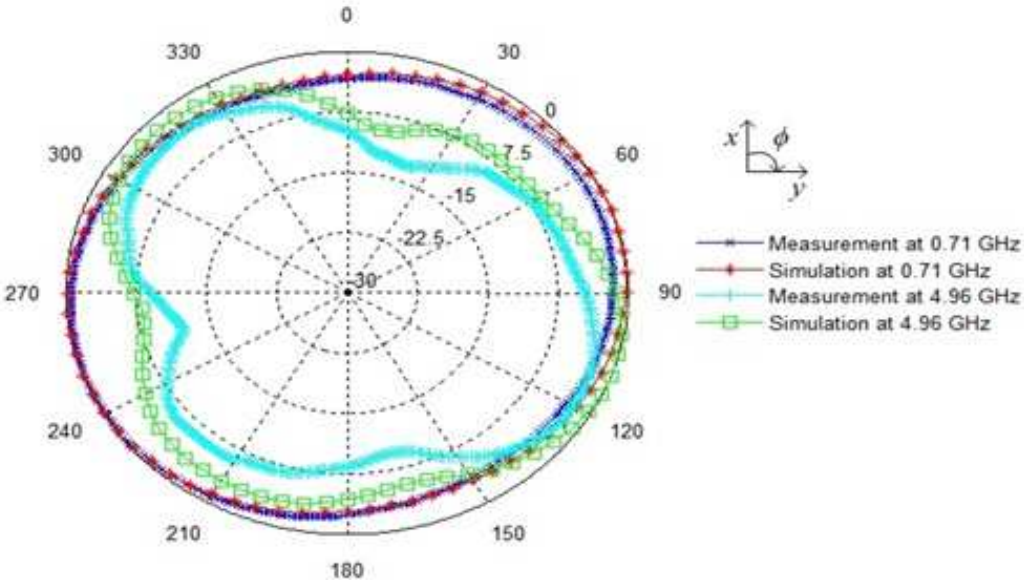

Fig. 3.10: Simulated and measured total normalized electric field intensities of the antenna in xy plane.

3.6 Conclusion

A frequency reconfigurable electrically-small antenna with a high tunable frequency ratio of 7, between two frequencies bands (718 MHz and 4960 MHz), is presented for US Public Safety wireless communications. The reconfigurability is obtained using a single RF MEMS switch. Both modes of operation are jointly optimized and the impedance and radiation pattern measurements are characterized. The fabricated antenna shows good measured performances, which agree reasonably well with the simulations. The antenna achieves a reasonably wide measured bandwidth of 2.6% at 718MHz given its electrically-small lateral dimensions of $\lambda/10x\lambda/10$. The integrity of radiation patterns is also reasonably maintained in both modes of operation. Work is under way to further improve the radiation integrity over the reconfigurable modes of operation.

Chapter 4

MEMS Integrated Three-Band PIFA for Public Safety Bands

4.1 Antenna's Architecture and Operation

Chapter 4 presents another version of the design presented in Chapter 3 with the same size but with an additional band of operation. The geometry shown in Fig. 4.1 is a frequency reconfigurable antenna capable of switching between the public safety bands 843.5 MHz to 872.2 MHz (mode 1_1), 799.3 to 819 MHz (mode 1_2), and 4900 MHz (mode 2).

The additional feature of this antenna is providing an extra band in 800MHz range is obtained by adding 2 MEMS switches: one on the top patch and the other one on the modified reconfigurable ground plane. Hence, the antenna would have three modes of operations: mode 1_1 (843.5 to 872.2 MHz), mode 1_2 (799 to 819 MHz) , and mode 2 (4900 MHz). The ground plane geometry is changed properly to satisfy the above mentioned frequency bands for all the three modes of operation. The meander is used to increase the electrical length of the antenna for mode 1_1. The meander is connected and disconnected from the reconfigurable ground plane for switching between the three modes of operation, mode 1_1, mode 1_2, and mode 2. An additional switch is presented on the meander to reconfigure between mode 1_1 and mode 1_2. The top patch extension is used to improve the impedance matching in mode 2. The band width in this design is wider in all three modes than the bandwidth in the previous version with two switches (presented in Chapter 3). There is always a trade-off between the number of MEMS switches needed to the number of PS bands that can be covered by a frequency reconfigurable antenna. Although the design presented in Chapter 3 can cover three PS bands with wider BWs when compared to the design in Chapter 2, it requires two more additional MEMS switches to accomplish this task.

The critical parameters of this design, shown in Fig. 4.2, are as follows: L_{gs} and W_{gs}

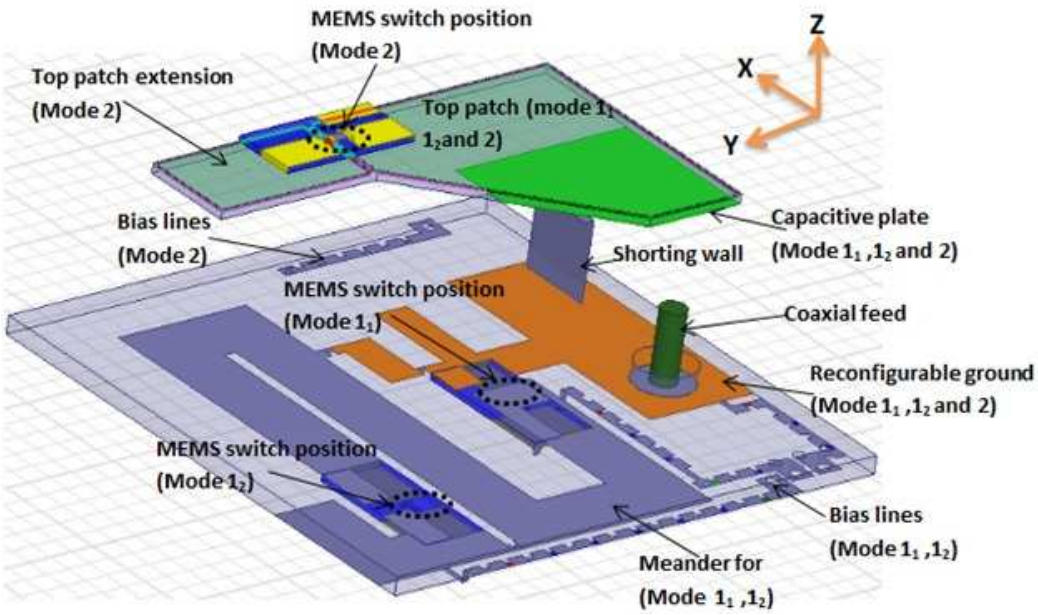

Fig. 4.1: The 3D view of the proposed three mode frequency reconfigurable PIFA.

are the length and the width of the ground substrate, respectively; W_g and L_g show the width and the length of the reconfigurable ground plane; L_T and W_T show the length and the width of the T-shape ground plane; L_A represents the length of the T-shaped arm; L_{4900} shows the resonant length for mode 2 operation; $L_{800} + L_{840}$ and L_{840} represent the resonant lengths for mode 1_1 and mode 1_2, respectively; W_{sp1}, W_{sp2}, W_{sp3} show the spacing between the meander; W_m shows the width of the meander; L_p and W_p are the length and width of the top patch element; A and B show the tapering length; L_{ext} represents the length of the extension that added to the top patch; L_c and W_c are the length and width of the capacitor plate; a shows the tapering length on the capacitor; and W_{sh} shows the width of the shorting plane; the resistors are used to ground the meander.

The antenna has been designed using Ansys HFSS v13. A hard-wired model has been fabricated and measured, and the corresponding reflection coefficient plots are shown in the Fig. 4.3. In a hard-wired model, copper strips are used to open and short the switches instead of actual MEMS. In the next step MEMS switches would replace the copper strips to perform switching. As is evident from the plots in Figs. 4.3 - 4.5, the measured results are in reasonable agreement with the simulation results. The unwanted resonances present

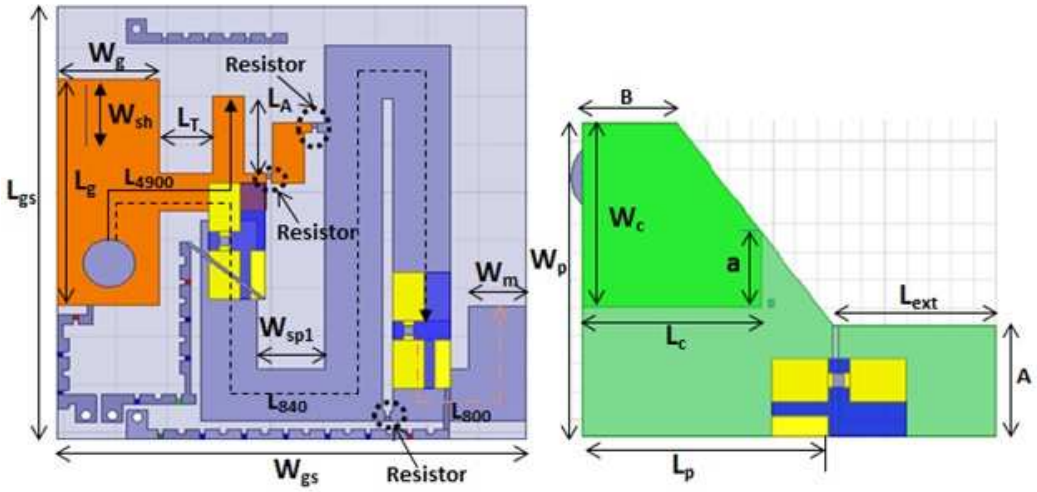

Fig. 4.2: The schematics of the RF MEMS integrated antenna depicting the critical design parameters.

in the simulation results are due to the numerical errors in HFSS.

The design has been fabricated and been sent for MEMS integration to Cornell University of New York, but due to some priority of other designs the MEMS will be integrated and measured later on. The above results are from the hard-wired measurement which has been done at Micro/Nano lab of USU, and as can be observed from the figures above, the measurement results are in a reasonably well agreement with the simulation results from HFSS version 13th.

4.2 Conclusion and Future Work

To unlock the additional features of a frequency reconfigurable antenna, number of MEMS switches used in the design needs to be increased. The design with three switches works in three modes of operations, mode 1_1 (843.5 to 872.2 MHz), mode 1_2 (799 to 819 MHz), and mode 2 (4900 MHz). MEMS integration and radiation pattern measurement efforts are still under progress. This paper represented three frequency reconfigurable MEMS integrated PIFA antenna designs, the first design was a combination of two frequency reconfigurable MEMS integrated PIFAS for public safety bands of the United States with a 12 cm x 12 cm in size, works in two modes of operation: 778 MHz to 838 MHz in mode 1 which

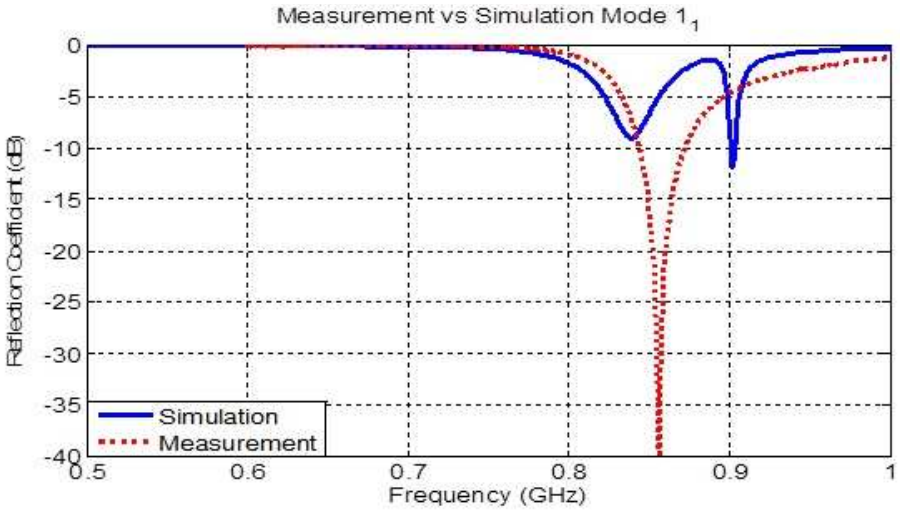

Fig. 4.3: Simulated and measured reflection coefficient plots of the presented antenna in mode 1_1.

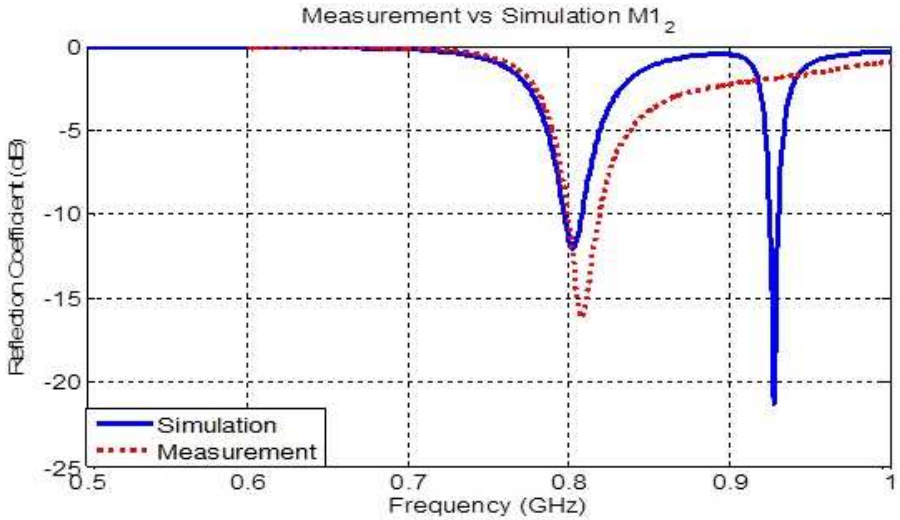

Fig. 4.4: Simulated and measured reflection coefficient plots of the presented antenna in mode 1_2.

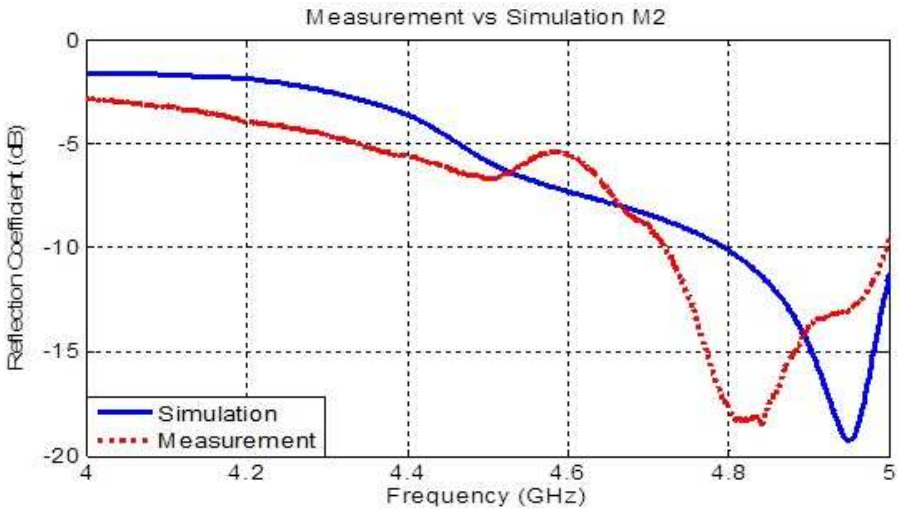

Fig. 4.5: Simulated and measured reflection coefficient plots of the presented antenna in mode 2.

is a 60 MHz bandwidth; and 4900 MHz in mode 2; and three MEM switches were used to reconfigure between the two bands of operation, as the size of the antenna in today's wireless communication is more considerable. The second design was an electrically-small frequency reconfigurable MEMS integrated PIFA with two modes of operation, the central frequency in mode 1 is 718 MHz with a bandwidth of 20 MHz, and 223 MHz bandwidth in mode 2, with electrical length of $\lambda/10$ by $\lambda/10$, the antenna was fabricated and measured and the measurement results versus the simulation results were in a reasonably well agreement with each other. To get more bandwidths the third antenna has been designed, fabricated, and measured, working in three modes of operation with resonances at 804 MHz, 840 MHz, and 4900 MHz with 19 MHz, 20 MHz, and 223 MHz bandwidths in mode 1_1, mode 1_2, and mode 2, respectively. The future work on these designs will be to further reduce the size of the antenna for bandwidth enhancement and add parasitic layer on the top for beam tilting purposes.

References

[1] G. Rebeiz and H. J. W. Gabriel, "Rf mems: theory, design and technology," *Electronics Letters, IEEE*, vol. 20, no. 23, 2003.

[2] F. Wang, Z. Du, Q. Wang, and K. Gong, "Enhanced-bandwidth pifa with t-shaped ground plane," *Electronics Letters*, vol. 40, no. 23, pp. 1504–1505, 2004.

[3] A. Khoshniat, H. Mopidevi, and B. Cetiner, "Broadband capacitively fed tapered type pifa with modified ground plane," *Electronics Letters*, vol. 46, no. 7, pp. 474–475, 2010.

[4] G. Vandenbosch, "Capacitive matching of microstrip antennas," *Electronics letters*, vol. 31, no. 18, pp. 1535–1536, 1995.

[5] C. Byung, D. Ju, and D. Hyumg, "Tapered type pifa design for mobile phones at 1800 mhz," in *Vehicular Technology Conference, IEEE*, pp. 1012–1014, 2003.

[6] B. Cetiner, H. Jafarkhani, J. Qian, H. Yoo, A. Grau, and F. De Flaviis, "Multifunctional reconfigurable mems integrated antennas for adaptive mimo systems," *Communications Magazine, IEEE*, vol. 42, no. 12, pp. 62–70, 2004.

[7] K. Boyle and P. Steeneken, "A five-band reconfigurable pifa for mobile phones," *Antennas and Propagation, IEEE Transactions*, vol. 55, no. 11, pp. 3300–3309, 2007.

[8] B. Cetiner, G. Crusats, L. Jofre, and N. Biyikli, "Rf mems integrated frequency reconfigurable annular slot antenna," *Antennas and Propagation, IEEE Transactions*, vol. 58, no. 3, pp. 626–632, 2010.

[9] J. McLean, "A re-examination of the fundamental limits on the radiation q of electrically small antennas," *Antennas and Propagation, IEEE Transactions*, vol. 44, no. 5, p. 672, 1996.